

Supporting Information

Manipulating Transfer and Separation of Photocarriers in Monolayer WS₂ via CdSe Quantum Dots Doping

Qiushi Feng,¹ Yuanzheng Li,¹ Fei Gao,¹ Ying Sun,¹ Jiaxu Yan,¹ Weizhen Liu,^{1} Haiyang Xu,^{1*} and Yichun Liu¹*

¹Centre for Advanced Optoelectronic Functional Materials Research and Key Laboratory of UV-Emitting Materials and Technology, Northeast Normal University, Ministry of Education, Changchun 130024, China

*Email address: wzliu@nenu.edu.cn, hyxu@nenu.edu.cn

Contents

Note 1 Preparation details of CVD-grown 1L-WS₂ flakes

Note 2 Preparation of CdSe@ZnS core@shell QDs

Note 3 PMMA assisted transfer process

Note 4 Mass-action-model

S1. LPCVD synthesis of large-area 1L-WS₂ flakes on the sapphire substrate

S2. Low-magnification TEM images and Size distribution of the synthesized QDs

S3. Illustration of the PMMA assisted transfer process

S4. AFM height scan of the prepared QDs on 1L-WS₂ flake

S5. High-resolution TEM image of bare CdSe QDs

S6. PL mappings of 1L-WS₂ emission for the 1L-WS₂ flake prior to and after the spin-coating of CdSe-QDs

S7. XPS spectra of Cd 3d and Se 3d core levels of 1L-WS₂/CdSe-QDs heterostructure

S8. Height profile images corresponding to Scanning Kelvin probe force microscopy (KPFM) measurement

S9. Photoresponsivity and specific detectivity calculated from the measured photocurrent

Table S1 Bi-exponential fitting results of each parameter for the CdSe-QDs PL lifetime

Table S2 Tri-exponential fitting results of each parameter for the 1L-WS₂ PL lifetime

Note 1 Preparation details of CVD-grown 1L-WS₂ flakes

The synthesis of 1L-WS₂ flakes by low pressure chemical vapor deposition (LPCVD) was carried out in a double body tube furnace (OTF-1200X-S2-50SL). As reaction sources, sulfur powder (Sigma-Aldrich, 99.99%, 1 g) and tungsten trioxide (WO₃) powder (Sigma-Aldrich, 99.98%, 5 mg) were placed in two separate quartz boats as shown in **Figure S1a**. Since WS₂ is difficult to grow due to the high melting points of WO₃ precursor, we added 15 mg of sodium chloride powder into WO₃ powder as flux.¹ Herein, a relatively high dosage of sulfur powder is used to ensure the full sulfurization of WO₃, which is beneficial to reduce the sulfur vacancies and improve the crystallinity of prepared samples. The sulfur powder was placed in the center of the low temperature tube furnace, upstream at a distance of 55 cm from the WO₃ powder which was put in the center of the high temperature tube furnace. Afterwards, *c*-plane (0001) sapphire substrates were placed downstream of the WO₃ powder with a separation of 0.5 cm. Before heating, the quartz tube was purged with ultrapure N₂ gas to exhaust any remnant air. And then, the furnace was rapidly heated to the preset temperatures (130 °C for the sulfur powder and 950 °C for the WO₃ powder respectively, in consideration of the simultaneous evaporation of these two precursors) under a constant flow rate of 50 sccm of N₂ gas. The reaction took place at low pressure 4.7 pa for 20 min during which the temperatures were held on. After that, the CVD system was naturally cooled down to room temperature under the protection of N₂ gas. The temperature profiles employed for formation of WS₂ with the target reaction temperature of 950 °C and 130 °C for two precursors are displayed in the **Figure S1b**.

Note 2 Preparation of CdSe@ZnS core@shell QDs

CdSe@ZnS core@shell QDs are synthesized by two step metal-organic chemical method.² First, Cadmium oleate ($\text{Cd}(\text{OA})_2$) and trioctylphosphine selenide (TOPSe) are selected as precursors to synthesize the core CdSe QDs. To obtain 1 mM $\text{Cd}(\text{OA})_2$ solution, cadmium oxide (CdO , 1 mM) and oleic acid (OA, 3 mM) were loaded into a 50 ml three-neck flask and heated to 200 °C under vacuum conditions. In another flask, 1 M TOPSe solution was prepared by reacting trioctylphosphine (TOP) with selenium powder at 50 °C. 10 ml of octadecene (ODE, 20 mM) and oleylamine (OLA, 20 mM) were added to the flask containing $\text{Cd}(\text{OA})_2$ solution after cooling to room temperature. When heating the above mixed solution to 350 °C, 2 ml of prepared TOPSe solution was rapidly injected into the vigorously stirred reaction mixture. Then numerous CdSe nanoparticles can be formed in a short time. To prevent continuous nucleation of CdSe nanoparticles, the temperature was rapidly decreased to 240 °C. The temperature was then slowly raised to 280 °C and maintained for 5 minutes to promote the growth of CdSe nanoparticles.

In the next step, 1 ml of bisdimethyldithiocarbamic acid zinc salt ($\text{Zn}(\text{DMTC})_2$, 1M) in octylamine was added into the above CdSe solutions at room temperature to coat ZnS layer on the core CdSe QDs. The temperature was slowly increased to 180 °C and maintained for 10 minutes to grow the ZnS shell. After cooling to room temperature, the solution was repeatedly treated with hexane and ethanol to separate the CdSe@ZnS QDs from the unreacted precursors. Then the CdSe@ZnS QDs were precipitated with excess acetone. Finally, the CdSe@ZnS QDs were highly soluble in toluene. The core and shell sizes of the synthesized QDs shown in **Figure S2** were characterized by TEM measurements, respectively.

Note 3 PMMA assisted transfer process

The 1L-WS₂ was transferred from the as-grown sapphire substrate to a TEM grid using polymethyl methacrylate (PMMA)-assisted wet transfer.³ A film of PMMA was spin-coated on the surface of 1L-WS₂ from a dilute solution (mass fraction 4% in acetone, 1000 rpm for 20 s). Then above sample was submerged in 2 mol/L sodium hydroxide (NaOH) solution and heated in 100 °C for 30 min to etch the oxide. After the substrate released strain, the PMMA/WS₂ film was floating on the surface of solution. Next, the PMMA/WS₂ film was transferred to the TEM grid. The film was allowed to dry for 6 h, and then the PMMA was removed in hot acetone and the substrate was rinsed with ethanol to further clean unpurified organic pollutants. The transfer of the 1L-WS₂ was finished after drying.

Note 4 Mass-action-model

The mass-action-model correlated with the charged trion is applied to calculate the net electron concentration N_e of 1L-WS₂, which is employed to estimate the doping level. Firstly, the populations of A exciton N_A and charged trion N_A^- from steady-states equation can be expressed as:⁴

$$N_A(n) = \frac{G}{\Gamma_{ex} + k_{tr}(n)} \quad (S1)$$

$$N_A^-(n) = \frac{k_{tr}(n)}{\Gamma_{tr}} \cdot \frac{G}{\Gamma_{ex} + k_{tr}(n)} \quad (S2)$$

where n represents the number of doping times, G stands for the optical generation rate of A exciton, $k_{tr}(n)$ is the formation rate of the charged trion from A exciton, Γ_{ex} and Γ_{tr} express the decay rate of A exciton and charged trion respectively. Secondly, the PL intensity proportional to the populations of the A exciton (charged trion) can be obtained as follows:

$$I_A(n) = \frac{AG\gamma_{ex}}{\Gamma_{ex} + k_{tr}(n)} \quad (S3)$$

$$I_A^-(n) = \frac{k_{tr}(n)}{\Gamma_{tr}} \cdot \frac{AG\gamma_{tr}}{\Gamma_{ex} + k_{tr}(n)} \quad (S4)$$

where coefficient A represents the collection efficiency of luminescence, γ_{ex} and γ_{tr} express the radiative recombination rate of the A exciton and charged trion respectively. According to previous reports, $\Gamma_{ex} = 0.002 \text{ ps}^{-1}$, $\Gamma_{tr} = 0.02 \text{ ps}^{-1}$ and $k_{tr}(0) = 0.5 \text{ ps}^{-1}$. The best fitting parameters γ_{ex}/γ_{tr} is 0.06.⁴ Thirdly, based on the above equations, the corresponding relation correlated with the net electron concentration N_e of 1L-WS₂ is shown below:⁵

$$\frac{N_A N_e}{N_A^-} = \left(\frac{16\pi m_A m_e}{h^2 m_A^-} \right) k_B T \exp\left(-\frac{E_b}{k_B T} \right) \quad (S5)$$

where k_B is the Boltzman constant, T is the temperature, E_b is the binding energy of charged trion near the band gap ($\sim 26 \text{ meV}$).⁶ The m_e , m_A and m_A^- represent the effective mass of electrons, an exciton and a charged trion respectively; m_e and m_h are

$0.44m_0$ and $0.45m_0$ where m_0 is a free electron mass.⁷ The effective mass of a neutral exciton m_A and a trion $m_{\bar{A}}$ can be calculated as $m_A = m_e + m_h = 0.89m_0$, $m_{\bar{A}} = 2m_e + m_h = 1.34m_0$. Finally, using these parameters, the spectral weight of I_A^-/I_{total} ($I_{total} = I_A^- + I_{\bar{A}}^-$) can be presented as:

$$\frac{I_A^-}{I_{total}} = \frac{\frac{\gamma_{tr}}{\gamma_{ex}} \cdot \frac{N_A^-}{N_A}}{1 + \frac{\gamma_{tr}}{\gamma_{ex}} \cdot \frac{N_A^-}{N_A}} \approx \frac{1.65 \times 10^{-14} N_e}{1 + 1.65 \times 10^{-14} N_e} \quad (S6)$$

Namely

$$N_e = \frac{x}{1.65(1-x)} \times 10^{14}, x = \frac{I_A^-}{I_{total}} \quad (S7)$$

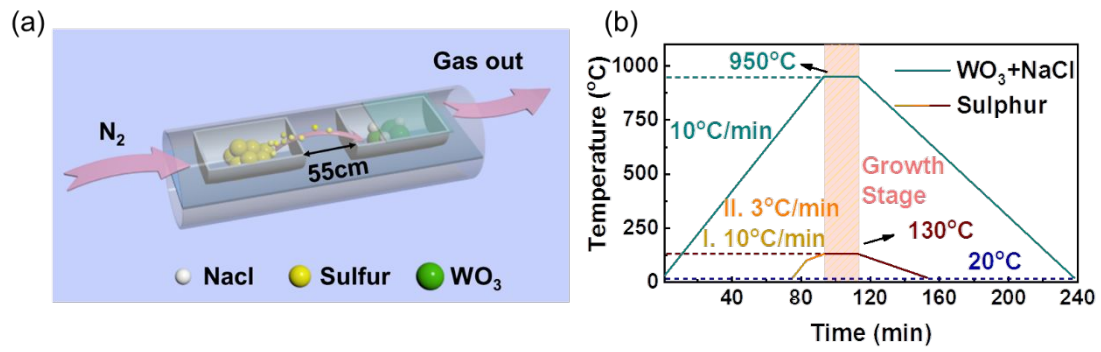


Fig. S1 LPCVD synthesis of large-area 1L- WS_2 flakes on the sapphire substrate. (a) Schematic presentation of the corresponding CVD experimental set-up. (b) The temperature profiles employed for formation of WS_2 with the target reaction temperature of 950 °C and 130 °C for WO_3 and Sulphur, respectively.

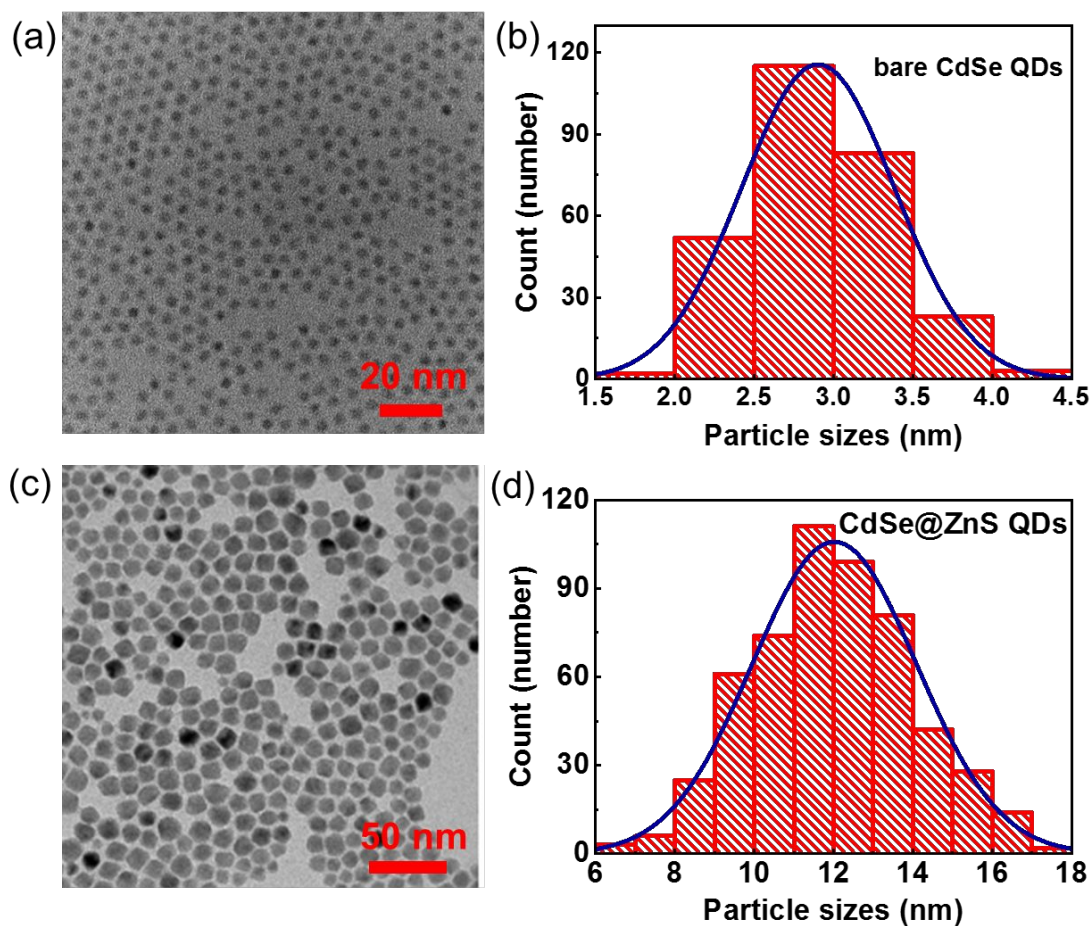


Fig. S2 (a) Low-magnification TEM image of bare CdSe QDs which are synthesized in the first step of **Note 2**. (b) Size distribution of the bare CdSe QDs in (a), solid line is a Gaussian fit centered at 3 nm. (c) Low-magnification TEM image of the CdSe@ZnS core@shell QDs which are synthesized in the second step of **Note 2**. (d) Size distribution of the core@shell QDs in (c), solid line is a Gaussian fit centered at 12 nm.

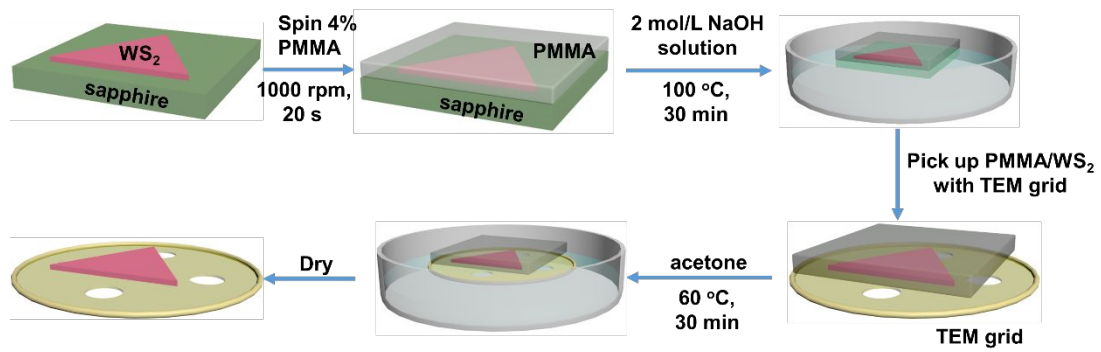


Fig.S3 Illustration of the PMMA assisted transfer process.

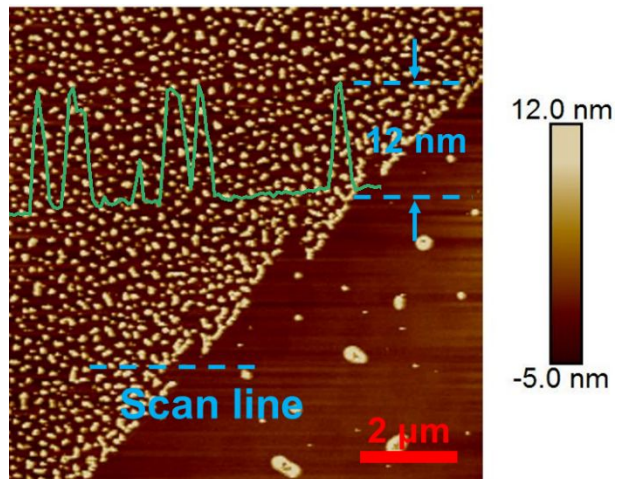


Fig. S4 Enlarged view of marginal region in **Fig. 2 (b)** for clarity; the aureate dots observed on the WS_2 flake are the spin-coated QDs; AFM height scan of the prepared QDs on 1L- WS_2 flake (along the blue dashed line), revealing the vertical height of these QDs is about 12 nm.

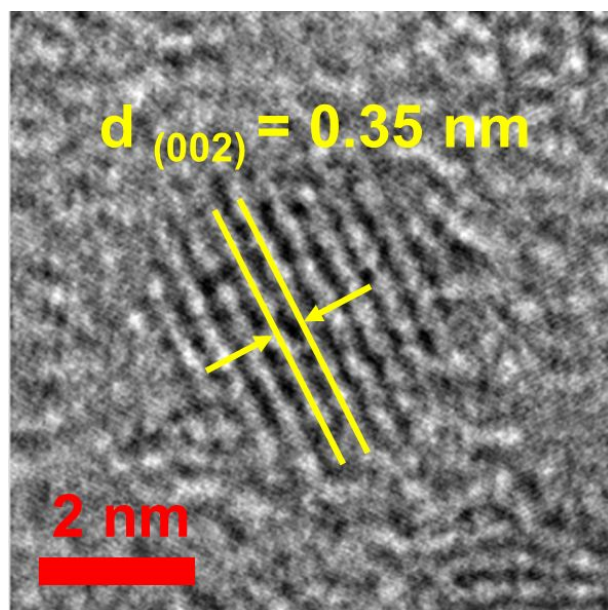


Fig. S5 High-resolution TEM image of bare CdSe QDs. Interplanar spacing of 0.35 nm corresponds to the (002) plane of CdSe.

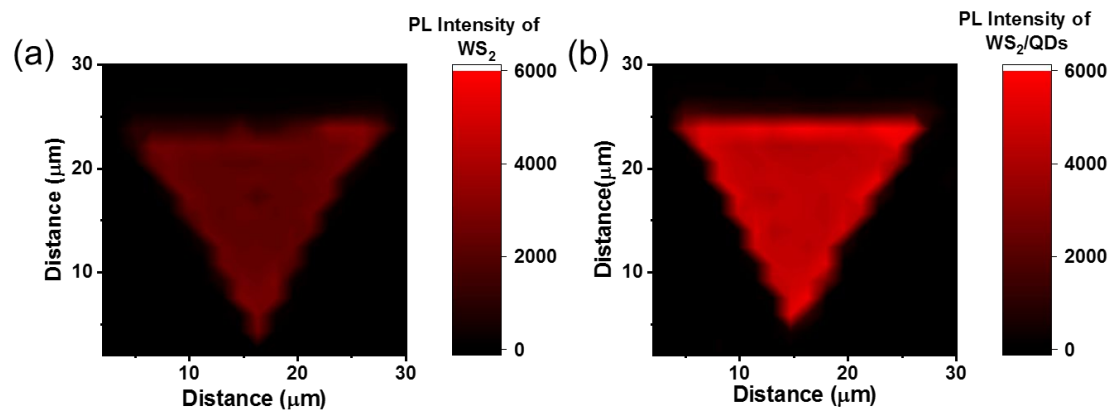


Fig.S6 PL mappings of 1L-WS₂ emission for the 1L-WS₂ flake prior to (a) and after the spin-coating of CdSe-QDs (b).

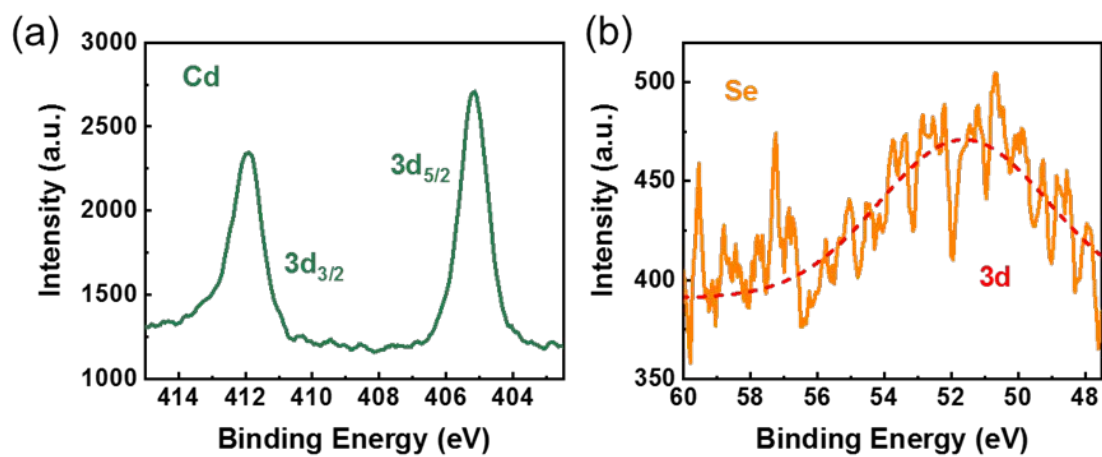


Fig.S7 XPS spectra of Cd 3d (a) and Se 3d (b) core levels of 1L-WS₂/CdSe-QDs heterostructure. Both XPS spectra are calibrated using the C 1s peak at 284.5 eV as a reference.

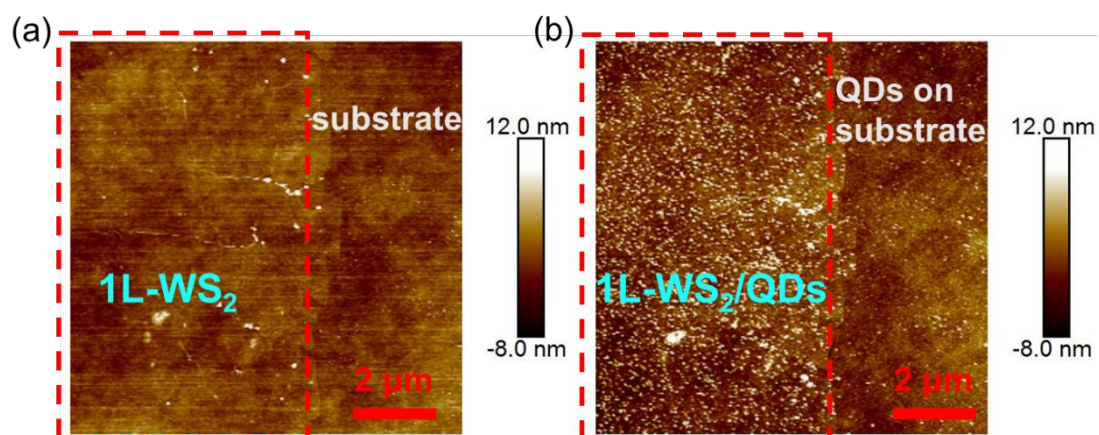


Fig. S8 Height profile images corresponding to Scanning Kelvin probe force microscopy (KPFM) measurements for 1L-WS₂ (a), 1L-WS₂/QDs heterostructure (b).

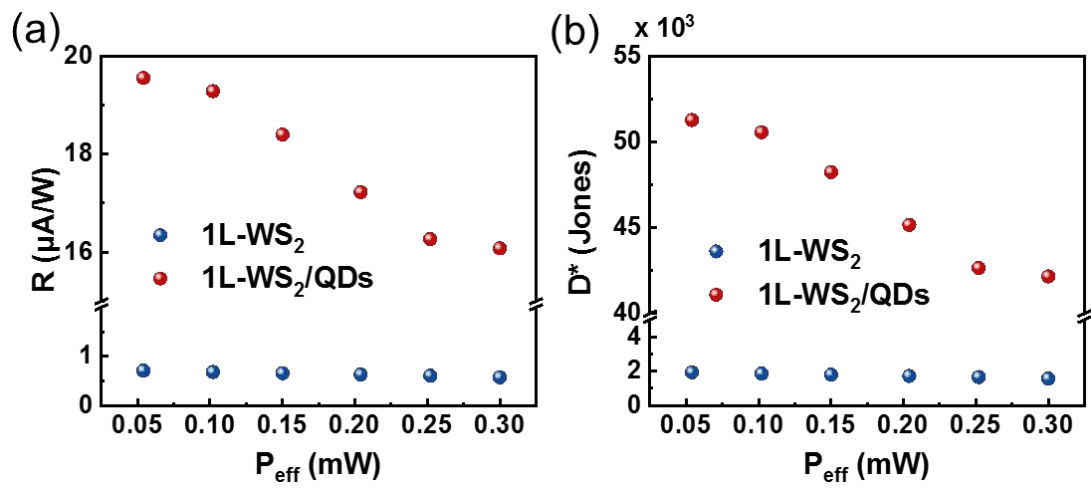


Fig. S9 Photoresponsivity (a) and specific detectivity (b) calculated from the measured photocurrent in **Fig. 6 b**.

Parameters	QDs	WS ₂ /QDs
A ₁	0.99	0.99
τ ₁ (ns)	0.79	0.62
A ₂	0.01	0.01
τ ₂ (ns)	21.07	10.46
τ _{eff} (ns)	5.71	2.55

Table S1 Bi-exponential fitting results of each parameter for the CdSe-QDs PL lifetime.

For CdSe-QDs with and without the 1L-WS₂ layer, we use a bi-exponential decay function ($I(t) = \sum a_i e^{-t/\tau_i}$, $i = 1, 2$) to fit the PL decay curve in **Figure 5a**. Herein, τ_1 and τ_2 correspond to the relatively fast radiative recombination process and the relatively slow surface-related recombination process, respectively.⁸ Then the effective lifetime ($\tau_{eff} = (A_1\tau_1^2 + A_2\tau_2^2)/(A_1\tau_1 + A_2\tau_2)$) of CdSe-QDs is displayed to describe the overall decay rate of excited-state carriers in CdSe-QDs. After contacting with 1L-WS₂, the PL lifetime of CdSe-QDs is significantly shortened (from 5.7 ns to 2.6 ns), which reflects a large portion of excitons are dissociated through interfacial electron transfer from QDs to 1L-WS₂.⁹

Parameters	WS ₂	WS ₂ /QDs
A ₁	0.20	0.12
τ ₁ (ps)	4.05	5.14
A ₂	0.79	0.87
τ ₂ (ps)	0.88	0.84
A ₃	0.01	0.01
τ ₃ (ps)	20.52	32.72
τ _{eff} (ps)	5.64	10.24

Table S2 Tri-exponential fitting results of each parameter for the 1L-WS₂ PL lifetime.

We also compare the PL lifetime of 1L-WS₂ before and after spin-coating CdSe-QDs in **Figure 5b**, which can be well fitted by a tri-exponential decay function ($I(t) = \sum a_i e^{-t/\tau_i}$, $i = 1, 2, 3$). Herein, τ_1 and τ_2 correspond respectively to relatively fast recombination process (e.g. non-radiative recombination related with Auger scattering or defect process), and τ_3 corresponds to relatively slow radiative recombination process (see **Table S2**).¹⁰ Furthermore, the effective lifetime 1L-WS₂ can be obtained by a formula of $\tau_{eff} = (A_1\tau_1^2 + A_2\tau_2^2 + A_3\tau_3^2)/(A_1\tau_1 + A_2\tau_2 + A_3\tau_3)$. For 1L-WS₂, the τ_{eff} is 5.6 ps, while it prolongs to 10.3 ps after spin-coating CdSe-QDs. The enhanced lifetime of 1L-WS₂ is mainly due to re-absorption of the fluorescence from excited CdSe-QDs, although the electron injection will shorten part of the lifetime.¹¹

References

- (1) Li, S.; Wang, S.; Tang, D.-M.; Zhao, W.; Xu, H.; Chu, L.; Bando, Y.; Golberg, D.; Eda, G., Halide-assisted atmospheric pressure growth of large WSe₂ and WS₂ monolayer crystals. *Appl. Mater. Today* **2015**, *1*, 60-66.
- (2) Chae, W.-S.; Ung, T. D. T.; Nguyen, Q. L., Time-resolved photoluminescence and photostability of single semiconductor quantum dots. *Adv. Nat. Sci-Nanosci.* **2013**, *4*, 045009.
- (3) Liu, K. K.; Zhang, W.; Lee, Y. H.; Lin, Y. C.; Chang, M. T.; Su, C. Y.; Chang, C. S.; Li, H.; Shi, Y.; Zhang, H.; Lai, C. S.; Li, L. J., Growth of large-area and highly crystalline MoS₂ thin layers on insulating substrates. *Nano Lett.* **2012**, *12*, 1538-1544.
- (4) Tao, Y.; Yu, X.; Li, J.; Liang, H.; Zhang, Y.; Huang, W.; Wang, Q. J., Bright monolayer tungsten disulfide via exciton and trion chemical modulations. *Nanoscale* **2018**, *10*, 6294-6299.
- (5) Rivera, A. M.; Gaur, A. P. S.; Sahoo, S.; Katiyar, R. S., Studies on chemical charge doping related optical properties in monolayer WS₂. *J. Appl. Phys.* **2016**, *120*, 105102.
- (6) Zhu, B.; Chen, X.; Cui, X., Exciton binding energy of monolayer WS₂. *Sci. Rep.* **2015**, *5*, 9218.
- (7) Ramasubramaniam, A., Large excitonic effects in monolayers of molybdenum and tungsten dichalcogenides. *Phys. Rev. B* **2012**, *86*, 115409.
- (8) Morello, G.; Anni, M.; Cozzoli, P.; Manna, L.; Cingolani, R.; De Giorgi, M., The Role of Intrinsic and Surface States on the Emission Properties of Colloidal CdSe and CdSe/ZnS Quantum Dots. *Nanoscale Res. Lett.* **2007**, *2*, 512-514.

- (9) Wu, H.; Kang, Z.; Zhang, Z.; Zhang, Z.; Si, H.; Liao, Q.; Zhang, S.; Wu, J.; Zhang, X.; Zhang, Y., Interfacial Charge Behavior Modulation in Perovskite Quantum Dot-Monolayer MoS₂ 0D-2D Mixed-Dimensional van der Waals Heterostructures. *Adv. Funct. Mater.* **2018**, *28*, 1802015.
- (10) Li, H.; Zheng, X.; Liu, Y.; Zhang, Z.; Jiang, T., Ultrafast interfacial energy transfer and interlayer excitons in the monolayer WS₂/CsPbBr₃ quantum dot heterostructure. *Nanoscale* **2018**, *10*, 1650-1659.
- (11) Huo, C.; Liu, X.; Wang, Z.; Song, X.; Zeng, H., High-Performance Low-Voltage-Driven Phototransistors through CsPbBr₃-2D Crystal van der Waals Heterojunctions. *Adv. Opt. Mater.* **2018**, *6*, 1800152.